RNA binding kinase UHMK1 regulates therapy induced metabolic adaptation in BRAF^{V600} melanoma

Lorey K Smith[1], Tiffany Parmenter[1], Margarete Kleinschmidt[1], Eric P Kusnadi[1], Jian Kang[1], Claire A Martin[1], Peter Lau[1,2], Teresa Ward[1], Aparna D Rao[1,2], Emily J Lelliott[1,2], Karen E Sheppard[1,2,3], Rodney J Hicks[1,2], Tony Tiganis[1,2,4], Kaylene J Simpson[1,2], Carleen Cullinane[1,2], Vihandha O Wickramasinghe[1,2], Richard B Pearson[1,2,3], Grant A McArthur[1,2,5]

1. Cancer Research Division, Peter MacCallum Cancer Centre, Australia.
2. Sir Peter MacCallum Department of Oncology, University of Melbourne, Australia.
3. Department of Biochemistry and Molecular Biology, University of Melbourne, Australia.
4. Department of Biochemistry and Molecular Biology, Monash University, Australia.
5. Department of Medicine, St. Vincent's Hospital, University of Melbourne, Australia.

Corresponding author: Professor Grant McArthur (grant.mcarthur@petermac.org)

Highlights

- Selective mRNA transport and translation regulates BRAF inhibitor sensitivity in BRAF^{V600} melanoma cells.
- BRAF targeted therapy reprograms metabolism via selective mRNA transport and translation.
- RNA binding kinase UHMK1 binds to mRNA encoding metabolic proteins and regulates their transport and translation following BRAF inhibition.
- Genetic inactivation of UHMK1 delays resistance to BRAF+MEK inhibition *in vivo.*

Summary

Despite the success of therapies targeting oncogenes in cancer, clinical outcomes are limited by drug adaptation and resistance. BRAF inhibition in melanoma results in multiple cellular adaptations that precede resistant disease, including altered metabolism. Here, we use a genome-wide RNAi screen to identify mRNA transport and translation as regulators of metabolic response and adaptation following BRAF inhibition in melanoma cells. Mechanistically, we demonstrate the RNA binding kinase UHMK1 interacts with mRNAs that encode metabolic proteins and selectively controls their transport and translation. Importantly, genetic inactivation of UHMK1 delays resistance to BRAF and MEK combination therapy *in vivo*. Our data support a model wherein selective mRNA transport and translation is activated in response to therapeutic stress and contributes to metabolic adaptation underpinning therapeutic response. Inhibition of this process may extend efficacy of targeted therapies in oncogene driven cancers that rely on RAS-MAPK signaling networks.

Introduction

Therapeutic adaptation is a multifaceted process that if overcome offers the potential for significant improvement in clinical outcomes for patients treated with targeted therapies. Maximising inhibition of oncogenic signaling has been the prevailing paradigm for improving antitumor responses to targeted therapies. This concept is exemplified in melanoma where maximal suppression of BRAF-MEK signaling using combination therapy has extended median survival to over 24 months from a historical base of less than 12 months (Larkin et al., 2014; Robert et al., 2015). Despite this, development of resistance remains a challenge for patients with advanced melanoma, and significantly, more than 20 mechanisms of resistance have been identified in patients progressing on targeted therapy (Lim et al., 2017). This highlights the need to improve therapeutic response before mutational resistance emerges. Prior to relapse, acquisition of a drug tolerant state occurs during early adaptive responses to BRAF and MEK targeted therapy in melanoma (Menon et al., 2015; Rambow et al., 2018; Sharma et al., 2010; Su et al., 2017), and it has been proposed that non-mutational mechanisms underpinning this adaptability may provide new targets to improve therapeutic efficacy.

Altered metabolism is a hallmark of cancer that has been intensely investigated over the last decade. How therapy reprograms metabolism and the role this plays during the adaptive response and development of resistance has received much less attention. In the setting of melanoma, we have previously shown that $BRAF^{V600}$ inhibitor sensitivity correlates with glycolytic response in pre-clinical (Parmenter et al., 2014) and clinical studies (McArthur et al., 2012). BRAF inhibition (BRAFi) also renders $BRAF^{V600}$ melanoma cells addicted to oxidative phosphorylation (OXPHOS) by releasing BRAF mediated inhibition of a MITF-PGC1A-OXPHOS pathway (Haq et al., 2013). This unleashes adaptive mitochondrial reprogramming, ultimately facilitating drug tolerance likely by compensating for suppressed glycolysis. Consistent with these observations, a “nutrient-starved” cell state emerges during the early drug adaptation phase following combined BRAF and MEK inhibition *in vivo*, and critically, cells appear to transition through this adaptive state as they acquire resistance (Rambow et al., 2018). Clinically, PGC1α (a biomarker for elevated OXPHOS) is induced in $BRAF^{V600}$ melanoma patients treated with BRAFi, either alone (Haq et al., 2013) or in combination with MEK inhibitors

(Gopal et al., 2014), whilst tumors that relapse following MAPK inhibitor treatment display an elevated mitochondrial biogenesis signature (Zhang et al., 2016). Together, these data suggest that maximal suppression of glycolysis and concurrent inhibition of adaptive mitochondrial metabolism may lead to improved therapeutic outcomes and interfere with drug adaptation following BRAF and MEK targeted therapy. Notably, however, early results emerging from clinical trials of mitochondrial inhibitors such as biguanides have been largely disappointing (Kordes et al., 2015), and recent preclinical analyses support the concept that mechanisms underlying metabolic plasticity and adaptation may represent a more attractive therapeutic target (Hulea et al., 2018).

Here, we examined metabolic reprogramming in the therapeutic adaptation phase prior to acquired resistance using a genome-wide RNAi screen. This systematic approach uncovered mRNA transport and translation pathways as critical regulators of metabolic response and adaptation following BRAFi in $BRAF^{V600}$ melanoma cells. Mechanistically, we demonstrate that metabolic adaptation is associated with selective mRNA transport and translation of metabolic proteins critical to BRAF inhibitor sensitivity and resistance, including glucose transporters and OXPHOS enzymes. This translational reprograming is mediated by the RNA binding kinase UHMK1 that is required for mitochondrial flexibility in response to BRAFi and controls the abundance of metabolic proteins through the export and translation of the mRNA that encode them. Importantly, genetic inactivation of UHMK1 increases sensitivity to BRAF and MEK combination therapy and delays resistance *in vivo*. Together, our data support a model wherein selective mRNA transport and translation contributes to the metabolic adaptation that underpins therapy induced cancer cell plasticity, and suggests inhibition of this pathway may delay resistance to MAPK pathway targeted therapies.

Results

RNA binding, transport and translation pathways regulate metabolic response to BRAF inhibition.

To identify new regulators of metabolic response to BRAF inhibition (BRAFi), we performed a genome wide RNAi glycolysis screen in $BRAF^{V600}$ melanoma cells treated

with the BRAFi vemurafenib (Vem)(Figure 1A). Lactate is routinely used to measure glycolysis and can be readily detected in growth medium using a lactate dehydrogenase (LDH) enzyme based reaction. Cell number and viability were determined from nucelar DAPI staining using automated image analysis. For the screen, cells were first transfected with the human siGENOME SMARTPool library and subsequently treated with DMSO or a sub maximal dose of Vem (~IC25)(Figure 1A). We chose a 48hr treatment which is within the window of metabolic adaptation following BRAFi, whereby maximal suppression of glycolysis (Parmenter et al., 2014) and adaptive mitochondrial reprogramming ((Haq et al., 2013; Zhang et al., 2016); Figure S1A) is observed. Notably, increased expression of SLC7A8 (LAT2), a biomarker of a drug tolerant "starved" melanoma state following BRAFi+MEKi *in vivo* (Rambow et al., 2018), was also observed (Figure S1B). Transfection of WM266.4 $BRAF^{V600}$ cells with siRNA targeting polo-like kinase 1 (PLK1; death control) and pyruvate dehydrogenase kinase 1 (PDK1; glycolysis control) were used to define the dynamic range of the screening assays (Figure 1B), and notably, glycolysis was significantly more attenuated in Vem+siPDK1 cells compared to either Vem or siPDK1 alone, providing proof of principle for the major aim of the screen.

In the absence of drug, viability was impaired by depletion of 622 genes (Table S1) that formed a robust network (Figure S2A) enriched for regulators of cell cycle, translation and the ribosome (Figure S2B), processes previously shown to be critical for melanoma survival (Boussemart et al., 2014; Feng et al., 2015; Kardos et al., 2014). Glycolysis was reduced by depletion of 164 genes (Table S2), and as expected these genes were enriched with annotations associated with metabolism (Figure S2C and Table S2). To identify genes that regulate viability and glycolytic response to BRAFi, genes were grouped based on fold change data for each parameter in DMSO versus Vem treatment conditions (see supplementary information). This analysis identified 717 genes (Table S3) that were enriched for MAPK and GPCR signaling, and histone methylation, consistent with previous studies investigating BRAFi resistance (Figure 1C & Figure S2D)(Johannessen et al., 2013). However, the most striking feature of the gene set was RNA binding and transport, which was associated with 4 of the top 20 annotations ranked by P-value (Figure 1C & Table S3), with a total of 12 annotations associated with

these pathways enriched in the dataset (Table S3). The identification of RNA binding and transport proteins in our screen was particularly intriguing given these proteins are emerging as key determinants of gene expression programs activated in response to microenvironmental stress (El-Naggar and Sorensen, 2018). This group also included components of the EIF3 and EIF4F translation initiation complexes, and genes that regulate selective mRNA translation, thus also implicating mRNA translation in glycolytic responses to Vem. Notably, EIF4F has previously been reported as a nexus of resistance to MAPK pathway inhibitors in melanoma (Boussemart et al., 2014) thus further supporting performance of the screen. Comparative network analysis revealed 3 major hubs connect the viability and glycolysis networks; 1. GPCR signaling, 2. MAPK signaling, and 3. RNA transport and translation (Figure 1D), suggesting these pathways may coordinately regulate metabolic and viability responses to BRAFi. Consistently, 7 of the RNA transport and translation genes also enhanced the effects of Vem on viability (Figure 1E). The major findings of the screen were confirmed using a secondary de-convolution screen, whereby four individual siRNA duplexes were assessed to determine reproducibility of gene knockdown phenotypes. Notably, multiple RNA transport and translation genes were validated by 2 or more duplexes (33%; Figure S2E). We next assessed changes in expression of the RNA binding, transport and translation gene set using a published transcriptomic analysis of melanoma patients progressing after treatment with BRAF+/-MEK inhibitor treatment (Hugo et al., 2015). Strikingly, this analysis revealed that 18 out of 23 (78%) RNA transport and translation genes were upregulated in 10-36% of patients progressing on BRAF+/-MEK inhibitor treatment (Figure 1F & Table S4). By way of comparison, PGC1A was upregulated in 43% of patients in this dataset, whilst other previously documented biomarkers of acquired resistance to MAPK pathway inhibition in patients, c-MET and AXL, were upregulated in 33% of patients (Figure 1F). Viewed together, these large scale and unbiased analyses support a role for RNA binding, transport and translation pathways in regulation of metabolic response and viability following BRAFi.

Depletion of the RNA transport and translation regulators UHMK1 and YBX1 sensitizes BRAF^{V600} melanoma cells to BRAFi.

Among these RNA binding proteins we further investigated the roles of U2AF homology motif kinase 1 (UHMK1) and Y-box binding protein 1 (YBX1) in regulation of metabolic response to BRAFi in a panel of BRAF mutant melanoma cell lines (Figure 2 & S3). Both these proteins regulate cellular adaptation via selective RNA transport and translation (Cambray et al., 2009; El-Naggar et al., 2015; Evdokimova et al., 2009; Kosnopfel et al., 2018; Pedraza et al., 2014) thus we hypothesized they may also regulate metabolic reprogramming via RNA processing in the context of adaptation following BRAFi. First, UHMK1 and YBX1 knockdown was confirmed using qRT-PCR and western blotting (Figure S3A). Because UHMK1 lacks a specific antibody for the endogenous human protein, we also confirmed increased levels of its key target p27, which is degraded following phosphorylation by UHMK1 (Boehm et al., 2002). siUHMK1+Vem and siYBX1+Vem treated cells showed more attenuated lactate production (Figure 2A), glucose utilization (Figure 2B), extracellular acidification rates (ECAR; Figure 2C), and expression of glycolysis regulators (Figure 2D & S3B) when compared to BRAFi alone, indicating a reduction in glycolysis. Analysis of pyruvate dehydrogenase (PDH) activity, a mitochondrial gatekeeper enzyme that converts pyruvate into acetyl co-A, revealed increased phosphorylation in both siUHMK1+Vem and siYBX1+Vem treated cells (Figure 2E), consistent with reduced PDH activity. A more marked reduction in cell number (Figure S3C) and cell proliferation (Figure 2F & S3D-F) was also observed in siUHMK1+Vem and siYBX1+Vem cells compared to Vem alone, and conversely, an increase in cell death was observed in 3 out of 4 cell lines (Figure 2G). Together these data identify an important role for the UHMK1 and YBX1 RNA transport and selective translation pathways in glycolytic, proliferative, and viability responses to BRAFi in $BRAF^{V600}$ melanoma cells. Of note, UHMK1 depletion elicited a more pronounced phenotype in BRAFi treated cells in the majority of these assays. Moreover, UHMK1 was of most interest given it is the only known kinase to contain a classical RNA binding domain (the U2AF homology domain), suggesting it may function as a critical hub linking cell signaling and RNA processing to metabolic reprogramming. The kinase domain of UHMK1 shows limited homology to known kinases, however a K54A mutation in the putative active site extinguishes kinase activity (Maucuer et al., 1997). In order to establish the contribution of UHMK1 kinase activity in BRAFi response, we first genetically inactivated UHMK1 using CRISPR-Cas9 and confirmed increased sensitivity

of A375 cells to BRAFi (Figure 2H & S3G). Importantly this effect was rescued by expression of UHMK1-V5, but not the kinase dead K54A-V5 mutant (Figure 2H). UHMK1 expression and activity was confirmed using qRT-PCR and western blot analysis (Figure S3G). Viewed together, this data confirms a role for the kinase function of UHMK1 in therapeutic responses to BRAF inhibition in melanoma cells.

UHMK1 reprograms metabolism in response to BRAFi in BRAF^{V600} melanoma Cells.

We next investigated whether UHMK1 can also promote adaptive reprogramming of metabolism in response to BRAFi in melanoma cells. Due to cell death after 72hr treatment with Vem+siUHMK1 (Figure 2G), we assessed cells after 48hr which immediately precedes overt mitochondrial reprogramming (Figure S1A). Analysis of oxygen consumption rates (OCR) using Seahorse extracellular flux analysis (Figure 3A) revealed only modest effects on basal and maximal OCR (Figure 3B & C) in Vem+siUHMK1 treated cells. However, significant reductions in spare respiratory capacity (Figure 3D) and ATP production (Figure 3E) were observed, indicating a reduced ability to respond to changes in energy demand and suggesting that UHMK1 can promote mitochondrial flexibility in response to BRAFi. Impaired mitochondrial metabolism in Vem+siUHMK1 treated cells was not associated with reduced mitochondrial number (Figure 3F), moreover only modest effects on PGC1A mRNA expression was observed (Figure 3G). We also assessed expression of mitochondrial transcription factor A (TFAM), another key regulator of mitochondrial biogenesis, and again saw no evidence of a role for UHMK1 in its expression. Instead, analysis of OXPHOS protein levels following Vem treatment revealed increased expression of several OXPHOS proteins (NDUFB8, SDHB, UQCRC2, MTCO1), with the exception of ATP5A from complex V (Figure 3H), and importantly, this increase in OXPHOS proteins was UHMK1 dependent (Figure 3H). Together this data suggests that UHMK1 is required for regulation of oxidative metabolism following BRAFi by modulating OXPHOS protein expression independent of changes in the PGC1A- or TFAM- mitochondrial biogenesis transcription factor networks.

UHMK1 binds to mRNA encoding metabolic proteins and regulates their nuclear-cytoplasmic transport in BRAF^{V600} melanoma cells adapting to BRAFi.

To understand how UHMK1 regulates metabolic response and adaptation following BRAFi, we next employed a systematic approach to look at mRNA expression pathways from transport to translation. The effect of Vem and UHMK1 knockdown on nuclear-cytoplasmic mRNA transport was first assessed using RNA fluorescence *in situ* hybridization (FISH) with an oligo(dT) probe which specifically binds to poly(A)$^+$ pools of RNA (Figure 4A). In control conditions, the poly(A)$^+$ signal was predominantly equal between the nucleus and cytoplasm (Figure 4A), however in contrast, depletion of the principal mRNA export factor NXF1 caused accumulation of the poly(A)$^+$ signal in the nucleus (Figure 4A-B). Notably, nuclear accumulation of poly(A)$^+$ mRNA was also observed in UHMK1 depleted cells, confirming a role for UHMK1 in mRNA transport in the context of melanoma cells. BRAFi also gave rise to a significant increase in the poly(A)$^+$ nuclear to cytoplasm ratio (Figure 4B), however no further change was observed in the siUHMK1+Vem and siNXF1+Vem treated cells.

The modest phenotype of UHMK1 compared to NXF1 depletion indicated a more selective role for UHMK1 in mRNA transport. To extend these observations, we next assessed nuclear-cytoplasmic transport of specific mRNA transcripts using qRT-PCR analysis of nuclear and cytoplasmic mRNA pools generated from subcellular fractionation. The fractionation was verified by monitoring levels of mRNA known to be enriched within the nucleus (metastasis associated lung adenocarcinoma transcript 1; MALAT1) and cytoplasm (ribosomal protein S14; RPS14)(Figure S4A). We focused on mRNA encoding core proteins that function in glycolysis (glucose transporter 1 (GLUT1), hexokinase 2 (HK2)) and OXPHOS (PGC1A, ubiquinol-cytochrome c reductase core protein 2 (UQCRC2; complex III), ATP synthase F1 subunit alpha (ATP5A; complex V)). Notably, reduced cytoplasmic mRNA (UQCRC2) and increased nuclear mRNA (GLUT1 & HK2; Figure 4C-D & S4B) was observed specifically in the Vem+siUHMK1 treated cells, indicating UHMK1 depletion results in defects in GLUT1, HK2, and UQCRC2 mRNA transport following BRAFi. In contrast, analysis of PGC1A and ATP5A transcripts revealed no significant change in mRNA distribution (Figure 4E & S4B), consistent with no evidence of a role for UHMK1 in their regulation from previous analyses (Figure 3).

Together, these observations suggest that UHMK1 can selectively regulate nuclear-cytoplasmic mRNA transport in the context of therapeutic adaptation in $BRAF^{V600}$ melanoma cells following BRAFi.

UHMK1 directly regulates localization and translation of specific mRNA transcripts by binding to mRNA (Cambray et al., 2009; Pedraza et al., 2014). To determine whether UHMK1 directly regulates mRNA encoding metabolic proteins following BRAF inhibition, we performed RNA immunoprecipitation (RNA-IP) assays using UHMK1-V5 expressing melanoma cells following DMSO or Vem treatment (Figure S4C). Strikingly, GLUT1, UQCRC2 and HK2 mRNA were not found in association with UHMK1-V5 in treatment naïve cells, however a significant increase in their association was observed following Vem treatment (Figure 4F & S4D). Further indicating specificity of the analysis and the pathway, no PGC1A mRNA could be detected in association with UHMK1 in any condition (Figure 4F). These data provide evidence that UHMK1 can directly regulate GLUT1, HK2, and UQCRC2 mRNA transport by physically associating with their mRNA, and strikingly, this association is induced by BRAFi.

UHMK1 associates with polysomes and regulates selective translation of mRNA encoding metabolic proteins following BRAFi.

To test the hypothesis that regulation of mRNA transport by UHMK1 selectively promotes translation of metabolic proteins following BRAFi, we next characterized the translational response of UHMK1 target genes following BRAFi. First, we isolated mRNA bound to ribosomes using poly-ribosome (polysome) profiling (Figure 5A). Cell lysates were fractionated on a sucrose density gradient to isolate mRNA or proteins in sub-polysome (mRNP complexes and 40S, 60S, and 80S monomer peaks) or actively translating polysome (3 or more ribosomes) fractions (Gandin et al., 2014). Global polysome profiles generated from control treated A375 cells revealed a high basal rate of translation, and strikingly, this was potently suppressed by BRAFi for either 24 or 40 hours (Figure 5B). In contrast, analysis of the UHMK1 target gene UQCRC2 revealed redistribution of its mRNA from untranslated sub-polysome fractions following 24hr Vem treatment to actively translating polysome fractions 40hr post treatment (Figure 5C), independent of changes in total mRNA levels (Figure 5D). Notably, translational

inhibition of a housekeeping gene NONO was maintained throughout the treatment (Figure S5A), moreover, no change in ATP5A (Figure 5C) or PGC1A (Figure S5A) mRNA translation efficiency was observed throughout the treatment. Together this data supports selective regulation of UQCRC2 mRNA translation following BRAFi, independent from changes in transcription or mRNA stability. We next extended this analysis to UHMK1 glycolytic targets, reasoning translational reprogramming may also underlie UHMK1's role in mediating reduction in glycolysis following BRAFi. Despite a significant reduction in total mRNA levels (Figure 5D), GLUT1 mRNA was present predominantly in polysome fractions in all treatment conditions (Figure 5C-D) consistent with the phenomena of "translational buffering", whereby the rate of mRNA translation efficiency is maintained despite a decrease in total mRNA levels (McManus et al., 2014). This observation suggests that any GLUT1 mRNA remaining in cells following BRAFi is translated at high efficiency. Although HK2 mRNA translation initially decreased following 24hr Vem treatment, a redistribution to heavy polysome fractions was observed after 40hr. Overall, this analysis supports a model whereby a highly selective translation program regulates mRNA encoding metabolic proteins in response to therapeutic stress in $BRAF^{V600}$ melanoma cells. To directly establish if UHMK1 plays a role in this process, we next analyzed *de novo* synthesis of proteins by giving a pulse with the methionine analogue L-azidohomoalanine (AHA), which is incorporated into all newly synthesized proteins, followed by biotin labeling, streptavidin pull-down, and western blot analysis (Figure 5Ei). Consistent with our polysome profile analysis, we observed a striking decrease in total AHA-labelled protein indicating a global inhibition of protein synthesis following 72hr Vem treatment (Figure 5Eii). In contrast, analysis of OXPHOS proteins following Vem treatment revealed a significant increase in *de novo* synthesis of UQCRC2 (Figure 5F), and significantly, increased synthesis of this OXPHOS protein was UHMK1 dependent. Again, supporting specificity of this pathway, no significant change in synthesis of ATP5A protein was observed (Figure 5F), consistent with polysome profiling of ATP5A mRNA (Figure 5C). Strikingly, we also observed that although GLUT1 protein synthesis was decreased following Vem treatment, this reduction was significantly more pronounced following UHMK1 knockdown (Figure 5F). This data suggests that UHMK1 depletion may cooperate with BRAFi to elicit a double-hit on the glycolysis pathway, whereby both GLUT1 mRNA

transcription and translation is concurrently switched off. Linking these observations to UHMK1's role in cellular responses to BRAFi, depletion of UQCRC2 and GLUT1 phenocopy UHMK1 knockdown whereby enhanced sensitivity to BRAFi was observed in cell proliferation assays (Figure S5C-E and (Parmenter et al., 2014)). However in contrast, no effect on Vem sensitivity was observed in the context of Vem+siATP5A treated cells (Figure S5E). Together, this data supports a model whereby UHMK1 regulates glycolysis and mitochondrial metabolism following BRAFi via mRNA transport and translation.

The mechanistic target of rapamycin (mTOR) pathway regulates translation and anabolic metabolism in response to nutrient supply (Ben-Sahra and Manning, 2017) and has been linked with a high OXPHOS phenotype in BRAF and MEK inhibitor resistance in melanoma cells (Gopal et al., 2014). Notably, although mTOR signaling was suppressed following BRAFi (Figure S6), no further changes to this pathway were observed following UHMK1 depletion, suggesting UHMK1 functions in an alternative pathway to modify mRNA translation during the early adaptation phase in cells treated with BRAFi. Differential association of mRNA processing and transport proteins with polysomes, and selective delivery of the transcripts they associate with, is another attractive hypothesis to explain translation of selective transcripts. To further explore the role of UHMK1 in adaptive programs following BRAF therapy, we precipitated proteins associated with polysomes using UHMK1-V5 expressing cells treated with DMSO or Vem (Figure 5G). As expected, small ribosomal protein RPS6 (a 40S ribosome component) was distributed in all fractions in control conditions, whilst large ribosomal protein RPL11 (an 80S ribosome component) was absent from early mRNP and 40S fractions. A significant reduction in the polysome to sub-polysome ratio was observed after Vem treatment (Figure 5H), consistent with global inhibition of translation (Figure 5B). Moreover, tubulin was restricted to sub-polysome fractions in both DMSO and Vem treated samples, further confirming specificity of the analysis (Figure 5G). In contrast, UHMK1-V5 protein was predominantly associated with sub polysome fractions in control conditions, however a redistribution of the protein to actively translating polysome fractions was observed following Vem treatment (Figure 5G-H). This data suggests that not only is UHMK1 recruited to polysomes in melanoma cells, but this association

increases in response to BRAF therapy. Consistent with these observations, immunofluorescence analysis revealed a dramatic re-localization of UHMK1 from the nucleus to cytoplasm in cells treated with Vem (Figure S7), and this was not associated with any change in UHMK1 protein levels (Figure S4Cii). Together this data supports a model whereby UHMK1 binds to mRNA and is translocated from the nucleus to the cytoplasm in response to BRAFi, where a proportion of the protein (~13%) associates with polysomes and participates in selective regulation of mRNA translation.

Genetic inactivation of UHMK1 sensitizes BRAF^{V600} melanoma cells to BRAF and MEK combination therapy *in vitro* and *in vivo*.

We were next interested in testing the hypothesis that UHMK1 depletion would improve response and delay resistance following treatment with the current standard of care for BRAF^{V600} melanoma patients, a BRAF+MEK inhibitor combination. First, we performed cell proliferation assays and observed more attenuated proliferation in cells treated with the siUHMK1+BRAFi+MEKi triple combination compared to the BRAFi+MEKi combination alone (Figure 6A-B). To assess the role of UHMK1 in therapeutic response to BRAFi+MEKi *in vivo*, we implanted A375 cells expressing CAS9 or two independent UHMK1 gRNA into NOD scid interleukin 2 gamma chain null (NSG) mice (Figure 6C-D). Importantly, increased sensitivity to BRAFi+MEKi combination therapy was observed in mice implanted with both UHMK1 knock out cell lines compared with mice implanted with the control cell line (Figure 6E), culminating in a highly significant increase in overall survival (Figure 6F). Viewed together, this data confirms a role for the UHMK1 RNA processing pathway in MAPK pathway inhibitor responses in BRAF^{V600} melanoma cells both *in vitro* and *in vivo*.

Altogether, our findings support a model wherein UHMK1 regulates metabolic response and adaptation following BRAFi by controlling the abundance of metabolic proteins through the selective transport and translation of the mRNA that encode them (Figure 7). Importantly, inactivation of this pathway significantly improved survival following combined BRAF and MEK inhibition *in vivo*, suggesting inactivation of this pathway may represent a new strategy to delay targeted therapy resistance in melanoma patients.

Discussion

Despite the success of therapies targeting oncogenes in cancer, clinical outcomes are limited by drug adaptation and acquired resistance (Hugo et al., 2015). An emerging phenomenon observed following inhibition of oncogenic signaling in a range of cancers is adaptive mitochondrial reprogramming and enhanced reliance on oxidative metabolism (Baenke et al., 2015; Biancur et al., 2017; Caino et al., 2015; Ghosh et al., 2015; Haq et al., 2013; Hernandez-Davies et al., 2015; Kluza et al., 2012). In pancreatic cancer models, cells that survive genetic inactivation of $KRAS^{G12D}$ display elevated mitochondrial metabolism, and treatment with an ATP synthase inhibitor delays relapse (Viale et al., 2014). Treatment of glioblastoma with PI3K inhibitors drives adaptive mitochondrial reprogramming that is associated with tumor cell invasion (Caino et al., 2015). Mitochondrial metabolism can also influence drug sensitivity, wherein analysis of melanoma patient samples linked mitochondrial gene expression signatures with intrinsic and adaptive resistance to BRAF and MEK inhibitors (Zhang et al., 2016). Inhibitors of oxidative metabolism, or the processes controlling adaptive mitochondrial reprogramming, are therefore attractive targets for combination therapy to circumvent acquired resistance before it can develop in a broad range of cancers. Here, we define a new mechanism of non-genomic drug adaptation whereby adaptive mitochondrial metabolism is regulated at the level of mRNA transport and translation and we identify the RNA binding kinase UHMK1 as central to this process. We propose inactivation of this pathway may represent a new strategy to delay targeted therapy resistance in melanoma patients.

mRNA translation has been implicated in responses to MAPK pathway inhibition and development of resistance in melanoma (Boussemart et al., 2014; Rapino et al., 2018). Here, we demonstrate that despite global suppression of translation during the early drug response phase, transcript selective translation reprograms mitochondrial metabolism through upregulation of OXPHOS proteins, and significantly, we show this is UHMK1 dependent. Importantly, upregulation of these mitochondrial proteins also occurs in melanoma patients progressing on BRAF and MEK targeted therapy (Zhang et al., 2016), linking these observations to resistance mechanisms in patients. Translational “buffering” (McManus et al., 2014) of glycolysis genes, whereby the rate

of mRNA translation efficiency is maintained despite a decrease in total mRNA levels, also emerged from our analysis, and *de novo* protein synthesis assays revealed GLUT1 translation was maximally suppressed following UHMK1 depletion in combination with BRAFi. Viewed in the context of previous studies describing transcriptional repression of GLUT1 following BRAFi , this data supports a model whereby UHMK1 depletion cooperates with BRAFi to elicit a double-hit on the glycolysis pathway, whereby both GLUT1 mRNA transcription and translation is concurrently switched off. Consistent with these observations, Rapino *et al* (Rapino et al., 2018) have recently described codon-specific translational reprogramming of glycolytic metabolism in melanoma, in this case mediated by translational regulation of HIF1A by uridine 34 (U_{34}) tRNA enzymes. Viewed together, these data suggest multiple mechanisms underpin transcript selective translational reprogramming of metabolism in cancer cells responding to oncogene targeted therapy. Interestingly, a recent report has also described translational reprogramming as a driver of phenotypic plasticity in the setting of melanoma cell invasion following glutamine deprivation (Falletta et al., 2017), indicating these pathways may also be part of a more general stress response activated by suppressed glycolytic metabolism when the BRAF oncogene is switched off.

However, in order for mRNA to be translated into protein it must first be exported from the nucleus and transported into the cytoplasm. This process is not always constitutive, as transcript selective RNA export pathways can regulate a range of biological processes including DNA repair, proliferation and cell survival (Wickramasinghe and Laskey, 2015). Interestingly, RNA binding proteins have recently been shown to regulate pro-oncogenic networks to control melanoma development (Cifdaloz et al., 2017), however their role in therapeutic response and oncogenic BRAF function has not been reported. Our work now implicates mRNA binding and transport as a driver of transcript selective translation following therapy, and we show that UHMK1 binds to mRNA encoding proteins relevant to patient response to MAPK pathway inhibitors and regulates their selective transport and translation. We suggest this mechanism allows cells to rapidly respond to cellular stimuli and stress such as nutrient deprivation. Interestingly, differential association of mRNA binding proteins with polysomes is one mechanism cells employ to rapidly regulate transcript selective translation (Aviner et al.,

2017), and association of UHMK1 protein with polysome fractions following BRAFi is consistent with this concept. Moreover, a recent proteomic analysis of polysomes revealed 45% of all proteins identified were annotated as RNA binding, and a significant proportion of these were regulators of RNA transport and processing (Aviner et al., 2017). Notably, 78% of the RNA transport and translation gene set identified by the screen were upregulated in 10 - 36% of patients progressing on BRAF +/- MEK inhibitor treatment. Importantly, this is comparable to documented biomarkers of acquired resistance to MAPK pathway inhibition in melanoma patients, including PGC1A (43%), AXL (33%) and c-MET (33%)(Hugo et al., 2015), indicating relevance of these findings to human disease. Further analyses are now required to identify gene expression signatures associated with dysregulation of UHMK1 and other selective RNA binding and transport pathways in order to comprehensively assess their role in early adaptation and acquired resistance to MAPK targeted therapies in cancer patients.

Our data suggests that UHMK1 inactivation does not influence selective RNA transport and translation through mTOR signaling, however UHMK1 activity is regulated by both AKT and ERK signaling in the context of growth factor stimulation (Lee and Kay, 2011). Further work is required to determine if UHMK1 may itself be a downstream target of the mTOR signaling network and function coordinately to control transcript selective translation in conditions of nutrient deprivation experienced by cancer cells following treatment with oncogene targeted therapy. Indeed, the eIF4E translation initiation factor, a component of the eIF4F translation complex subject to regulation by mTOR, has been implicated in mRNA processing, including nuclear-cytoplasmic mRNA export and transport (Bollmann et al., 2013; Culjkovic et al., 2005; Culjkovic-Kraljacic et al., 2012). Intriguingly, PGC1A expression and mitochondrial number remain unchanged by the BRAFi+siUHMK1 combination suggesting the UHMK1-RNA transport and translation pathway functions independently from the MITF-PGC1A-mitochondrial biogenesis pathway. Instead, a reduction in OXPHOS protein synthesis likely reduces the capacity of BRAFi+siUHMK1 treated cells to cope with glucose deprivation elicited by inhibition of BRAF signaling, a model supported by a reduction in spare metabolic capacity, and the ability of UQCRC2 knockdown to phenocopy UHMK1 depletion in combination with Vem.

Viewed collectively, our work supports a model wherein selective mRNA transport and translation is activated in response to therapeutic stress and contributes to metabolic reprogramming underpinning the adaptive therapeutic response. Our data demonstrate that the RNA binding kinase UHMK1 binds to mRNA encoding metabolic proteins critical to BRAFi response, and is required for their transport and translation following BRAFi. Inactivation of UHMK1 interferes with adaptive mitochondrial reprogramming following BRAFi, and critically, delays resistance and improves survival following combined BRAF and MEK inhibition *in vivo*. We propose that selective RNA transport and translation serves as a non-genomic mechanism of cancer cell adaptation and may provide a new target to interfer with drug adaptation and improve the efficacy of targeted therapies. We speculate this mechanism may also be relevant in broader oncogene driven cancer settings where responses to targeted therapies are blunted by phenotypic adaptation involving reprogrammed mitochondrial networks.

STAR Methods

Detailed methods are provided in the online version of this paper and include the following:

- Key resources table
- Contact for reagent and resource sharing
- Methods details
    - Cell lines and reagents
    - RNAi screen method
    - siRNA mediated gene knockdwon
    - Plasmids and establishment of stable cell lines
    - CRISPR-CAS9 genome editing
    - Lactate and Glucose utilization assay
    - Extracellular flux analysis
    - Dose respone and proliferation assays
    - Polysome profiling analysis
    - Protein-RNA immunoprecipitation
    - RNA-FISH

- RNA Fractionation
- RNA extraction and quantitative RealTime PCR (q-RT-PCR)
- Western immunoblotting
- In vivo mouse experiments

- Quantification and statistical analysis

Figure Legends

Figure 1. RNA binding, transport and translation pathways regulate metabolic response to BRAF inhibition.

A. Schematic summarising screen workflow (see STAR Methods). **B.** WM266.4 cells were transfected with the indicated siRNA and treated with DMSO or 300nM Vem for 48hr. Cell number was calculated using high content image analysis of DAPI stained cells (top panel) and growth media was collected for determination of lactate levels. Lactate absorbance values were normalised to cell number to determine lactate production per cell (bottom panel). Data is normalised to siOTP non-targeting (siOTP) transfected DMSO controls. Statistical significance was determined using a one-way ANOVA *** $p > 0.001$ (error bars = SEM, N=3). **C.** Functional annotation enrichment analysis was performed on 717 genes that enhanced the effects of Vem on lactate production (DMSO lactate per cell ratio < 0.5-fold change and Vem lactate per cell ratio > 0.5-fold change; see Table S1) using DAVID. Data is displayed as Log2 fold change versus -Log10 p-value. **D.** Network analysis was performed on 622 viability screen hits and 717 hits that enhanced the effects of Vem on lactate production using String (see Figure S1). Comparative network analysis was performed using Cytoscape, and hubs connecting the two networks are highlighted. **E.** Heat map displaying viability and lactate screening data for the indicated genes. **F.** Heatmap displaying percentage of melanoma patients with up-regulation of the indicated mRNA transport and translation genes on progression following treatment with MAPK pathway inhibitors (data sourced from (Hugo et al., 2015); see Table S4). See also Figure S1-2.

Figure 2. Depletion of the RNA transport and translation regulators UHMK1 and YBX1 sensitizes BRAF^{V600} melanoma cells to BRAFi

WM266.4 and A375 cells were transfected with the indicated siRNA and treated with DMSO or 300nM Vem for 48hr. Media was collected and lactate production **(A)** and

glucose utilisation **(B)** was determined. **C.** Extracellular acidification rate (ECAR) was determined using Seahorse Extracellular Flux Analysis. Data is normalised to cell number and expressed as fold change relative to siOTP DMSO controls (error bars = SEM, N=3). Effect of gene knockdown and Vem treatment on gene expression (**D)** and protein levels and activity **(E)** were determined using q-RT-PCR and western blot analysis, respectively. Gene expression analysis is expressed as Log2 fold change relative to siOTP DMSO controls. **F.** Cell proliferation was assessed in melanoma cells transfected with the indicated siRNA and treated with DMSO or 300nM Vem by monitoring confluency over time using an Incucyte automated microscope. A representative proliferation curve is shown (top panel) and average % confluency (normalised to T0) following 96hr treatment (bottom panel). **G.** Cell death was assessed in melanoma cells treated as in (F) using a Cell tox green cell death assay. Data is normalised to % confluency and expressed as fold change relative to siOTP DMSO controls (error bars = SEM, N=3). **H.** UHMK1 was genetically inactivated in A375 cells using CRISPR-Cas9, and a luciferase control, wild type UHMK1 or a K54A kinase dead mutant were ectopically expressed and sensitivity to Vem was assessed. Data is expressed as mean GI50 fold change relative to Cas9-Luciferase controls (error bars = SEM, N=4). Statistical significance was determined using a one-way ANOVA * $p > 0.05$, ** $p > 0.01$, *** $p > 0.001$, **** $p > 0.0001$. See also Figure S3.

Figure 3. UHMK1 reprograms mitochondrial metabolism in response to BRAFi. WM266.4 and A375 cells were transfected with the indicated siRNA and treated with DMSO or 300nM Vem for 48hr. **A.** Oxygen consumption rate (OCR) was determined using Seahorse Extracellular Flux Analysis and representative profiles for WM266.4 cells are shown (Oligo = oligomycin; FCCP = Carbonyl cyanide-4-(trifluoromethoxy) phenylhydrazone; Rot/Ant-A = rotenone + antimycin-A; representative of N=4). Effect of gene knockdown and Vem treatment on basal OCR **(B)**, max OCR **(C)**, spare respiratory capacity (SRC) **(D)**, and ATP production **(E)** was determined following treatment with mitochondrial inhibitors as indicated in **(A)**. Data is normalised to cell number and expressed as fold change relative to siOTP DMSO controls (error bars = SEM, N=4). **F.** Mitochondrial number was determined using high content image analysis of Mitotracker stained melanoma cells treated as indicated (error bars = SEM, N=3). **G.** Effect of gene knockdown and Vem treatment on expression of the indicated genes was determined

using q-RT-PCR. Data is expressed as Log2 fold change relative to siOTP DMSO controls. **H.** Whole cell lysates were analysed by western blot analysis for the indicated proteins. Data is representative of N=3 (SE=short exposure; LE=long exposure). Statistical significance was determined using a one-way ANOVA * $p > 0.05$, ** $p > 0.01$, *** $p > 0.001$, **** $p > 0.0001$. See also Figure S4.

Figure 4. UHMK1 binds to mRNA encoding metabolic proteins and promotes selective mRNA transport in BRAF^{V600} melanoma cells adapting to BRAFi.

A375 cells were transfected with the indicated siRNA and treated with DMSO or 1μM Vem for 48hr. **A.** RNA fluorescence *in situ* hybridization (FISH) using a poly(A)$^+$ RNA specific probe in A375 cells treated as indicated (representative of N=3). **B.** The nuclear to cytoplasm ratio of poly(A)$^+$ RNA was calculated using high content image analysis. Data is expressed as fold change relative to siOTP DMSO controls (error bars = SEM, N=3). **C-E.** Cell lysates were fractionated into nuclear and cytoplasmic pools of RNA and analyzed for the indicated genes using qRT-PCR. Whole cell lysates were used to assess total mRNA levels. **F.** RNA immunoprecipitation (RNA-IP) assays were performed in UHMK1-V5 expressing melanoma cells following treatment with DMSO or 1μM Vem for 48hr. The indicated mRNA transcripts were then analysed using qRT-PCR. Statistical significance was determined using a one-way ANOVA * $p > 0.05$, ** $p > 0.01$, *** $p > 0.001$, **** $p > 0.0001$. See also Figure S5.

Figure 5. UHMK1 associates with polysomes and regulates selective translation of mRNA encoding metabolic proteins following BRAFi

A. Schematic depicting the polysome profiling assay used to isolate mRNA bound to ribosomes. **B.** Polysome profiles of A375 cells treated with either DMSO or 1μM Vem for the indicated time on a 10-50% sucrose gradient (representative of N=3). **C.** Distribution of mRNA encoding the indicated genes was determined using qRT-PCR following 1μM Vem treatment for the indicated time. Data is representative of 2 independent experiments. **D.** mRNA levels of the indicated genes was determined using qRT-PCR analysis of total input mRNA samples (error bars = SEM, N=2). Statistical significance was determined using a one-way ANOVA * $p > 0.05$, ** $p > 0.01$, *** $p > 0.001$, **** $p > 0.0001$.**F.** Schematic depicting the AHA-based *de novo* protein synthesis assay and dot blot showing total AHA labelled protein obtained from siOTP or siUHMK1 transfected cells following treatment with DMSO or 1μM Vem for 72hr. Data is

representative of 3 independent experiments. **G.** Protein lysates from input samples (left panel) and following streptavidin IP (right panel) were assessed using western blot analysis of the indicated proteins. **H.** UHMK1-V5 expressing A375 cells were treated with DMSO or Vem for the indicated time, prior to polysome profiling. Representative profiles of 3 independent experiments are shown (Top panel). Proteins were precipitated from the sucrose fractions and the indicated proteins were analysed using western blotting (bottom panel). **I.** Protein levels in sub polysome (fractions 3-8) vs polysome (fractions 9-14) fractions were calculated using densitometry, and sub polysome to polysome ratios were calculated (error bars = SEM, N=3). Statistical significance was determined using a one-way ANOVA * $p > 0.05$, ** $p > 0.01$, *** $p > 0.001$, **** $p > 0.0001$. See also Figure S6-7.

Figure 6. Genetic inactivation of UHMK1 sensitizes BRAF^{V600} melanoma cells to BRAF and MEK combination therapy *in vitro* and *in vivo*.

Cell proliferation was assessed by monitoring confluency over time using an Incucyte automated microscope in melanoma cells transfected with the indicated siRNA and treated with DMSO, 300nM Vem, 10nM Cobi or Vem+Cobi. A representative proliferation curve **(A)** and average % confluency (normalised to T0) following 96hr treatment **(B)** is shown (error bars = SEM, N=3; top panel). **C.** Schematic of the *in vivo* drug sensitivity study. **D.** UHMK1 was genetically inactivated in A375 cells using CRISPR-Cas9 and UHMK1 KO was confirmed using qRT-PCR **(i)** and western blot analysis of UHMK1 target p27 **(ii). E.** Growth of A375-CAS9, A375-UHMK1-gRNA2 and A375-UHMK1-gRNA4 tumors treated with vehicle or dabrafenib and trametinib (Dab/Tram)(n=9 per group). **F.** Kaplan–Meier curve of data in **(E)** shows survival advantage where survival is defined as time to a tumor exceeding a volume of 1200mm^3. ****$P < 0.0001$ by Log-rank (Mantel-Cox) test.

Figure 7. RNA binding kinase UHMK1 reprograms metabolism in response to BRAFi via selective mRNA transport and translation.

Model depicting early metabolic response to BRAFi and its regulation by the UHMK1 mRNA transport and translation pathway.

Acknowledgements

We thank the following Peter MacCallum Cancer Centre core facilities: Victorian Centre for Functional Genomics (VCFG), Flow Cytometry and the Centre for Advanced Microscopy and Histology. The VCFG (K.J.S.) is funded by the Australian Cancer Research Foundation (ACRF), the Australian Phenomics Network (APN) through funding from the Australian Government's National Collaborative Research Infrastructure Strategy (NCRIS) program and the Peter MacCallum Cancer Centre Foundation. We thank Daniel Thomas, Jennii Luu, Kate Gould and Piyush Madhamshettiwar from the VCFG for technical and analytical assistance with the genome wide RNAi screen. We also thank Rachael Walker and Susan Jackson from the Translational Research Lab and Alison Slater from the Molecular Oncology Lab for assisting in the *in vivo* studies. This work was supported by grants from National Health and Medical Research Council of Australia (#1053792 and #1106576). A.R, P.L and E.L were supported by doctoral scholarships from the University of Melbourne and Cancer Therapeutics Cooperative Research Centre.

AUTHOR CONTRIBUTIONS

L.S, T.P, and G.M conceived and designed the project. L.S, T.P, K.J.S, and G.M designed experiments. L.S, T.P, M.K, E.K, J.K, T.W, and A.R conducted experiments. L.S and K.G performed data analysis. C.C and L.S designed and C.M, P.L, and E.L performed the *in vivo* experiments. V.W, R.P, T.T, K.E.S, C.C and R.J.H provided critical scientific input, protocols and/or reagents. L.S, V.W, R.P and G.M were involved in writing the manuscript, with all authors providing feedback.

DECLARATION OF INTERESTS

The authors declare no competing interests.

References

Aviner, R., Hofmann, S., Elman, T., Shenoy, A., Geiger, T., Elkon, R., Ehrlich, M., and Elroy-Stein, O. (2017). Proteomic analysis of polyribosomes identifies splicing factors as potential regulators of translation during mitosis. Nucleic acids research *45*, 5945-5957.

Baenke, F., Chaneton, B., Smith, M., Van Den Broek, N., Hogan, K., Tang, H., Viros, A., Martin, M., Galbraith, L., Girotti, M.R., *et al.* (2015). Resistance to BRAF inhibitors induces glutamine dependency in melanoma cells. Molecular oncology.

Ben-Sahra, I., and Manning, B.D. (2017). mTORC1 signaling and the metabolic control of cell growth. Current opinion in cell biology *45*, 72-82.
Biancur, D.E., Paulo, J.A., Malachowska, B., Quiles Del Rey, M., Sousa, C.M., Wang, X., Sohn, A.S.W., Chu, G.C., Gygi, S.P., Harper, J.W.*, et al.* (2017). Compensatory metabolic networks in pancreatic cancers upon perturbation of glutamine metabolism. Nature communications *8*, 15965.
Boehm, M., Yoshimoto, T., Crook, M.F., Nallamshetty, S., True, A., Nabel, G.J., and Nabel, E.G. (2002). A growth factor-dependent nuclear kinase phosphorylates p27(Kip1) and regulates cell cycle progression. The EMBO journal *21*, 3390-3401.
Bollmann, F., Fechir, K., Nowag, S., Koch, K., Art, J., Kleinert, H., and Pautz, A. (2013). Human inducible nitric oxide synthase (iNOS) expression depends on chromosome region maintenance 1 (CRM1)- and eukaryotic translation initiation factor 4E (elF4E)-mediated nucleocytoplasmic mRNA transport. Nitric oxide : biology and chemistry *30*, 49-59.
Boussemart, L., Malka-Mahieu, H., Girault, I., Allard, D., Hemmingsson, O., Tomasic, G., Thomas, M., Basmadjian, C., Ribeiro, N., Thuaud, F.*, et al.* (2014). eIF4F is a nexus of resistance to anti-BRAF and anti-MEK cancer therapies. Nature *513*, 105-109.
Buratti, E., and Baralle, F.E. (2011). TDP-43: new aspects of autoregulation mechanisms in RNA binding proteins and their connection with human disease. The FEBS journal *278*, 3530-3538.
Caino, M.C., Ghosh, J.C., Chae, Y.C., Vaira, V., Rivadeneira, D.B., Faversani, A., Rampini, P., Kossenkov, A.V., Aird, K.M., Zhang, R.*, et al.* (2015). PI3K therapy reprograms mitochondrial trafficking to fuel tumor cell invasion. Proceedings of the National Academy of Sciences of the United States of America *112*, 8638-8643.
Cambray, S., Pedraza, N., Rafel, M., Gari, E., Aldea, M., and Gallego, C. (2009). Protein kinase KIS localizes to RNA granules and enhances local translation. Molecular and cellular biology *29*, 726-735.
Cifdaloz, M., Osterloh, L., Grana, O., Riveiro-Falkenbach, E., Ximenez-Embun, P., Munoz, J., Tejedo, C., Calvo, T.G., Karras, P., Olmeda, D.*, et al.* (2017). Systems analysis identifies melanoma-enriched pro-oncogenic networks controlled by the RNA binding protein CELF1. Nature communications *8*, 2249.
Culjkovic, B., Topisirovic, I., Skrabanek, L., Ruiz-Gutierrez, M., and Borden, K.L. (2005). eIF4E promotes nuclear export of cyclin D1 mRNAs via an element in the 3'UTR. The Journal of cell biology *169*, 245-256.
Culjkovic-Kraljacic, B., Baguet, A., Volpon, L., Amri, A., and Borden, K.L. (2012). The oncogene eIF4E reprograms the nuclear pore complex to promote mRNA export and oncogenic transformation. Cell reports 2, 207-215.
El-Naggar, A.M., and Sorensen, P.H. (2018). Translational control of aberrant stress responses as a hallmark of cancer. The Journal of pathology 244, 650-666.
El-Naggar, A.M., Veinotte, C.J., Cheng, H., Grunewald, T.G., Negri, G.L., Somasekharan, S.P., Corkery, D.P., Tirode, F., Mathers, J., Khan, D., et al. (2015). Translational Activation of HIF1alpha by YB-1 Promotes Sarcoma Metastasis. Cancer cell 27, 682-697.
Evdokimova, V., Tognon, C., Ng, T., Ruzanov, P., Melnyk, N., Fink, D., Sorokin, A., Ovchinnikov, L.P., Davicioni, E., Triche, T.J., et al. (2009). Translational activation of snail1 and other developmentally regulated transcription factors by YB-1 promotes an epithelial-mesenchymal transition. Cancer cell 15, 402-415.
Falletta, P., Sanchez-Del-Campo, L., Chauhan, J., Effern, M., Kenyon, A., Kershaw, C.J., Siddaway, R., Lisle, R., Freter, R., Daniels, M.J., et al. (2017). Translation reprogramming is an evolutionarily conserved driver of phenotypic plasticity and therapeutic resistance in melanoma. Genes & development 31, 18-33.

Feng, Y., Pinkerton, A.B., Hulea, L., Zhang, T., Davies, M.A., Grotegut, S., Cheli, Y., Yin, H., Lau, E., Kim, H., et al. (2015). SBI-0640756 Attenuates the Growth of Clinically Unresponsive Melanomas by Disrupting the eIF4F Translation Initiation Complex. Cancer research 75, 5211-5218.
Gandin, V., Sikstrom, K., Alain, T., Morita, M., McLaughlan, S., Larsson, O., and Topisirovic, I. (2014). Polysome fractionation and analysis of mammalian translatomes on a genome-wide scale. Journal of visualized experiments : JoVE.
Ghosh, J.C., Siegelin, M.D., Vaira, V., Faversani, A., Tavecchio, M., Chae, Y.C., Lisanti, S., Rampini, P., Giroda, M., Caino, M.C., et al. (2015). Adaptive mitochondrial reprogramming and resistance to PI3K therapy. Journal of the National Cancer Institute 107.
Gopal, Y.N., Rizos, H., Chen, G., Deng, W., Frederick, D.T., Cooper, Z.A., Scolyer, R.A., Pupo, G., Komurov, K., Sehgal, V., et al. (2014). Inhibition of mTORC1/2 overcomes resistance to MAPK pathway inhibitors mediated by PGC1alpha and oxidative phosphorylation in melanoma. Cancer research 74, 7037-7047.
Haq, R., Shoag, J., Andreu-Perez, P., Yokoyama, S., Edelman, H., Rowe, G.C., Frederick, D.T., Hurley, A.D., Nellore, A., Kung, A.L., et al. (2013). Oncogenic BRAF regulates oxidative metabolism via PGC1alpha and MITF. Cancer cell 23, 302-315.
Hernandez-Davies, J.E., Tran, T.Q., Reid, M.A., Rosales, K.R., Lowman, X.H., Pan, M., Moriceau, G., Yang, Y., Wu, J., Lo, R.S., et al. (2015). Vemurafenib resistance reprograms melanoma cells towards glutamine dependence. Journal of translational medicine 13, 210.
Hugo, W., Shi, H., Sun, L., Piva, M., Song, C., Kong, X., Moriceau, G., Hong, A., Dahlman, K.B., Johnson, D.B., et al. (2015). Non-genomic and Immune Evolution of Melanoma Acquiring MAPKi Resistance. Cell 162, 1271-1285.
Hulea, L., Gravel, S.P., Morita, M., Cargnello, M., Uchenunu, O., Im, Y.K., Lehuede, C., Ma, E.H., Leibovitch, M., McLaughlan, S., et al. (2018). Translational and HIF-1alpha-Dependent Metabolic Reprogramming Underpin Metabolic Plasticity and Responses to Kinase Inhibitors and Biguanides. Cell metabolism 28, 817-832.e818.
Johannessen, C.M., Johnson, L.A., Piccioni, F., Townes, A., Frederick, D.T., Donahue, M.K., Narayan, R., Flaherty, K.T., Wargo, J.A., Root, D.E., et al. (2013). A melanocyte lineage program confers resistance to MAP kinase pathway inhibition. Nature 504, 138-142.
Kardos, G.R., Dai, M.S., and Robertson, G.P. (2014). Growth inhibitory effects of large subunit ribosomal proteins in melanoma. Pigment cell & melanoma research 27, 801-812.
Kluza, J., Corazao-Rozas, P., Touil, Y., Jendoubi, M., Maire, C., Guerreschi, P., Jonneaux, A., Ballot, C., Balayssac, S., Valable, S., et al. (2012). Inactivation of the HIF-1alpha/PDK3 signaling axis drives melanoma toward mitochondrial oxidative metabolism and potentiates the therapeutic activity of pro-oxidants. Cancer research 72, 5035-5047.
Kordes, S., Pollak, M.N., Zwinderman, A.H., Mathot, R.A., Weterman, M.J., Beeker, A., Punt, C.J., Richel, D.J., and Wilmink, J.W. (2015). Metformin in patients with advanced pancreatic cancer: a double-blind, randomised, placebo-controlled phase 2 trial. The Lancet Oncology 16, 839-847.
Kosnopfel, C., Sinnberg, T., Sauer, B., Busch, C., Niessner, H., Schmitt, A., Forchhammer, S., Grimmel, C., Mertens, P.R., Hailfinger, S., et al. (2018). YB-1 Expression and Phosphorylation Regulate Tumorigenicity and Invasiveness in Melanoma by Influencing EMT. Molecular cancer research : MCR 16, 1149-1160.
Larkin, J., Ascierto, P.A., Dreno, B., Atkinson, V., Liszkay, G., Maio, M., Mandala, M., Demidov, L., Stroyakovskiy, D., Thomas, L., et al. (2014). Combined vemurafenib and cobimetinib in BRAF-mutated melanoma. The New England journal of medicine 371, 1867-1876.

Lee, J.G., and Kay, E.P. (2011). PI 3-kinase/Rac1 and ERK1/2 regulate FGF-2-mediated cell proliferation through phosphorylation of p27 at Ser10 by KIS and at Thr187 by Cdc25A/Cdk2. Investigative ophthalmology & visual science 52, 417-426.
Lim, S.Y., Menzies, A.M., and Rizos, H. (2017). Mechanisms and strategies to overcome resistance to molecularly targeted therapy for melanoma. Cancer 123, 2118-2129.
Maucuer, A., Ozon, S., Manceau, V., Gavet, O., Lawler, S., Curmi, P., and Sobel, A. (1997). KIS is a protein kinase with an RNA recognition motif. The Journal of biological chemistry 272, 23151-23156.
McArthur, G.A., Puzanov, I., Amaravadi, R., Ribas, A., Chapman, P., Kim, K.B., Sosman, J.A., Lee, R.J., Nolop, K., Flaherty, K.T., et al. (2012). Marked, homogeneous, and early [18F]fluorodeoxyglucose-positron emission tomography responses to vemurafenib in BRAF-mutant advanced melanoma. Journal of clinical oncology : official journal of the American Society of Clinical Oncology 30, 1628-1634.
McManus, C.J., May, G.E., Spealman, P., and Shteyman, A. (2014). Ribosome profiling reveals post-transcriptional buffering of divergent gene expression in yeast. Genome research 24, 422-430.
Menon, D.R., Das, S., Krepler, C., Vultur, A., Rinner, B., Schauer, S., Kashofer, K., Wagner, K., Zhang, G., Rad, E.B., et al. (2015). A stress-induced early innate response causes multidrug tolerance in melanoma. Oncogene 34, 4545.
Parmenter, T.J., Kleinschmidt, M., Kinross, K.M., Bond, S.T., Li, J., Kaadige, M.R., Rao, A., Sheppard, K.E., Hugo, W., Pupo, G.M., et al. (2014). Response of BRAF-mutant melanoma to BRAF inhibition is mediated by a network of transcriptional regulators of glycolysis. Cancer discovery 4, 423-433.
Pedraza, N., Ortiz, R., Cornado, A., Llobet, A., Aldea, M., and Gallego, C. (2014). KIS, a kinase associated with microtubule regulators, enhances translation of AMPA receptors and stimulates dendritic spine remodeling. The Journal of neuroscience : the official journal of the Society for Neuroscience 34, 13988-13997.
Rambow, F., Rogiers, A., Marin-Bejar, O., Aibar, S., Femel, J., Dewaele, M., Karras, P., Brown, D., Chang, Y.H., Debiec-Rychter, M., et al. (2018). Toward Minimal Residual Disease-Directed Therapy in Melanoma. Cell 174, 843-855.e819.
Rapino, F., Delaunay, S., Rambow, F., Zhou, Z., Tharun, L., De Tullio, P., Sin, O., Shostak, K., Schmitz, S., Piepers, J., et al. (2018). Codon-specific translation reprogramming promotes resistance to targeted therapy. Nature 558, 605-609.
Robert, C., Karaszewska, B., Schachter, J., Rutkowski, P., Mackiewicz, A., Stroiakovski, D., Lichinitser, M., Dummer, R., Grange, F., Mortier, L., et al. (2015). Improved overall survival in melanoma with combined dabrafenib and trametinib. The New England journal of medicine 372, 30-39.
Sharma, S.V., Lee, D.Y., Li, B., Quinlan, M.P., Takahashi, F., Maheswaran, S., McDermott, U., Azizian, N., Zou, L., Fischbach, M.A., et al. (2010). A chromatin-mediated reversible drug-tolerant state in cancer cell subpopulations. Cell 141, 69-80.
Su, Y., Wei, W., Robert, L., Xue, M., Tsoi, J., Garcia-Diaz, A., Homet Moreno, B., Kim, J., Ng, R.H., Lee, J.W., et al. (2017). Single-cell analysis resolves the cell state transition and signaling dynamics associated with melanoma drug-induced resistance. Proceedings of the National Academy of Sciences of the United States of America 114, 13679-13684.
Vazquez, F., Lim, J.H., Chim, H., Bhalla, K., Girnun, G., Pierce, K., Clish, C.B., Granter, S.R., Widlund, H.R., Spiegelman, B.M., et al. (2013). PGC1alpha expression defines a subset of human melanoma tumors with increased mitochondrial capacity and resistance to oxidative stress. Cancer cell 23, 287-301.

Viale, A., Pettazzoni, P., Lyssiotis, C.A., Ying, H., Sanchez, N., Marchesini, M., Carugo, A., Green, T., Seth, S., Giuliani, V., et al. (2014). Oncogene ablation-resistant pancreatic cancer cells depend on mitochondrial function. Nature 514, 628-632.
Wickramasinghe, V.O., and Laskey, R.A. (2015). Control of mammalian gene expression by selective mRNA export. Nature reviews Molecular cell biology 16, 431-442.
Zhang, G., Frederick, D.T., Wu, L., Wei, Z., Krepler, C., Srinivasan, S., Chae, Y.C., Xu, X., Choi, H., Dimwamwa, E., et al. (2016). Targeting mitochondrial biogenesis to overcome drug resistance to MAPK inhibitors. The Journal of clinical investigation 126, 1834-1856.

Figure 1. RNA binding, transport and translation pathways regulate metabolic response to BRAF inhibition.

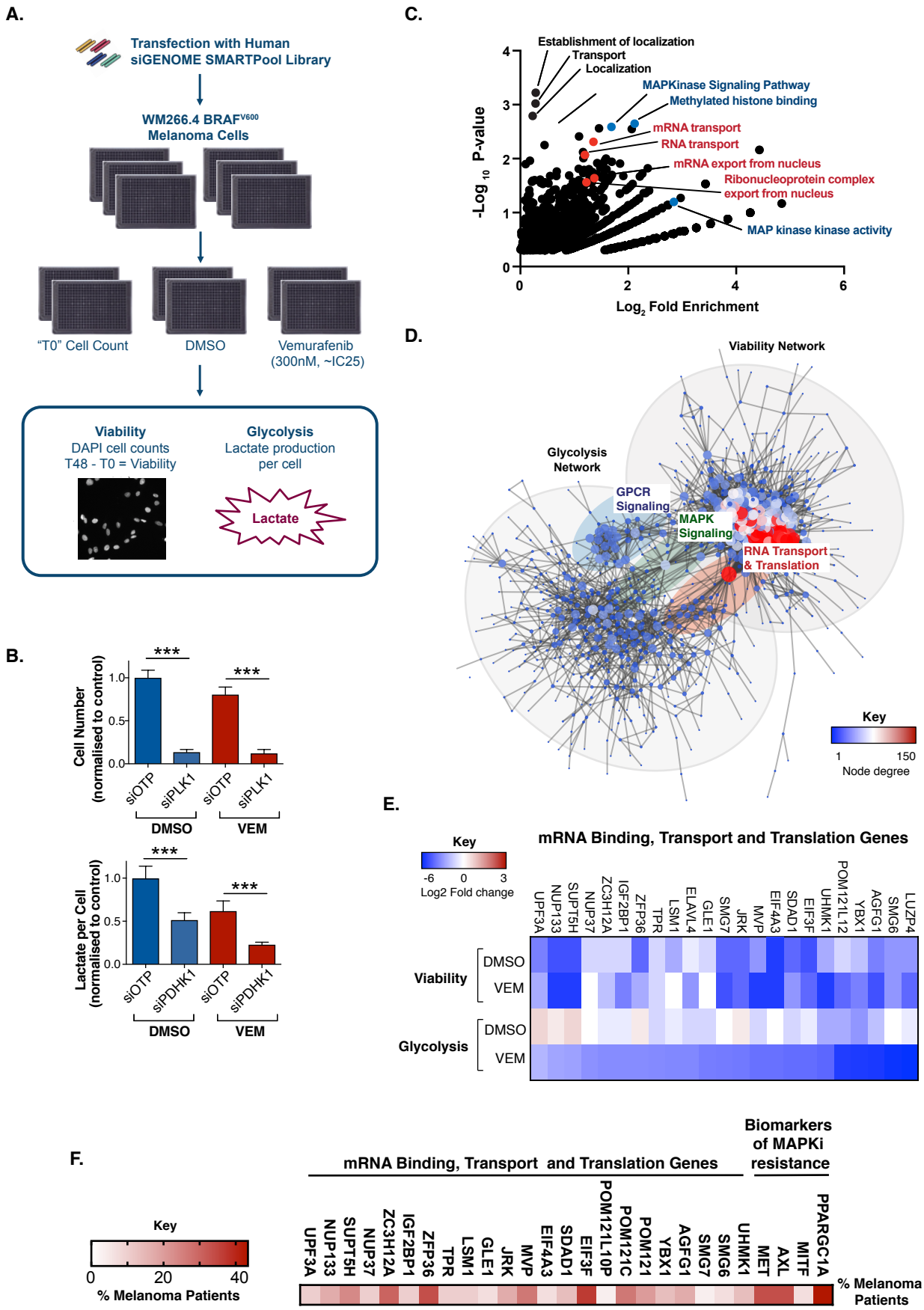

Figure 2. Depletion of UHMK1 and YBX1 sensitizes BRAF^{V600} melanoma cells to BRAF inhibition.

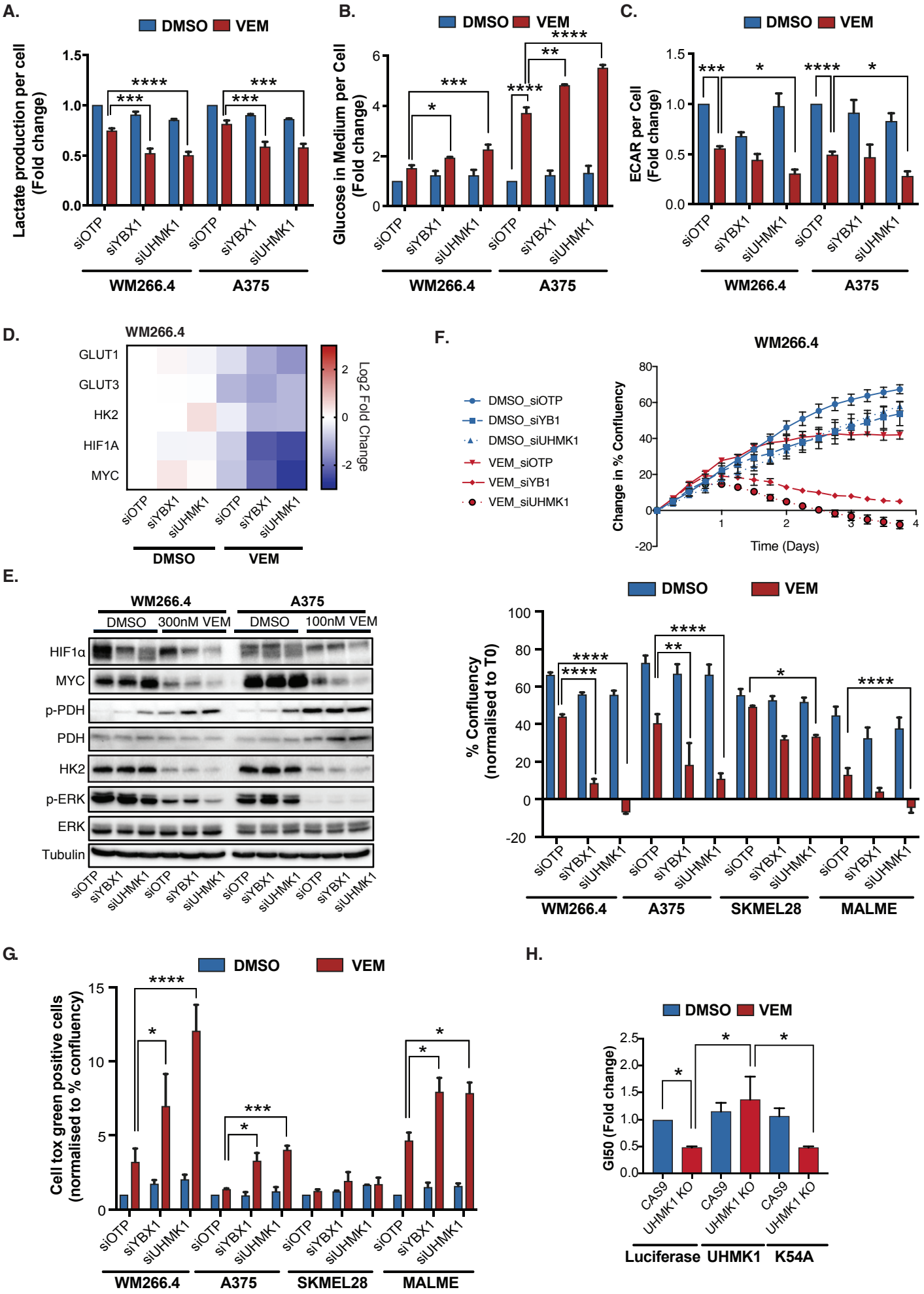

Figure 3. UHMK1 reprograms metabolism in response to BRAFi in BRAF^{V600} melanoma cells.

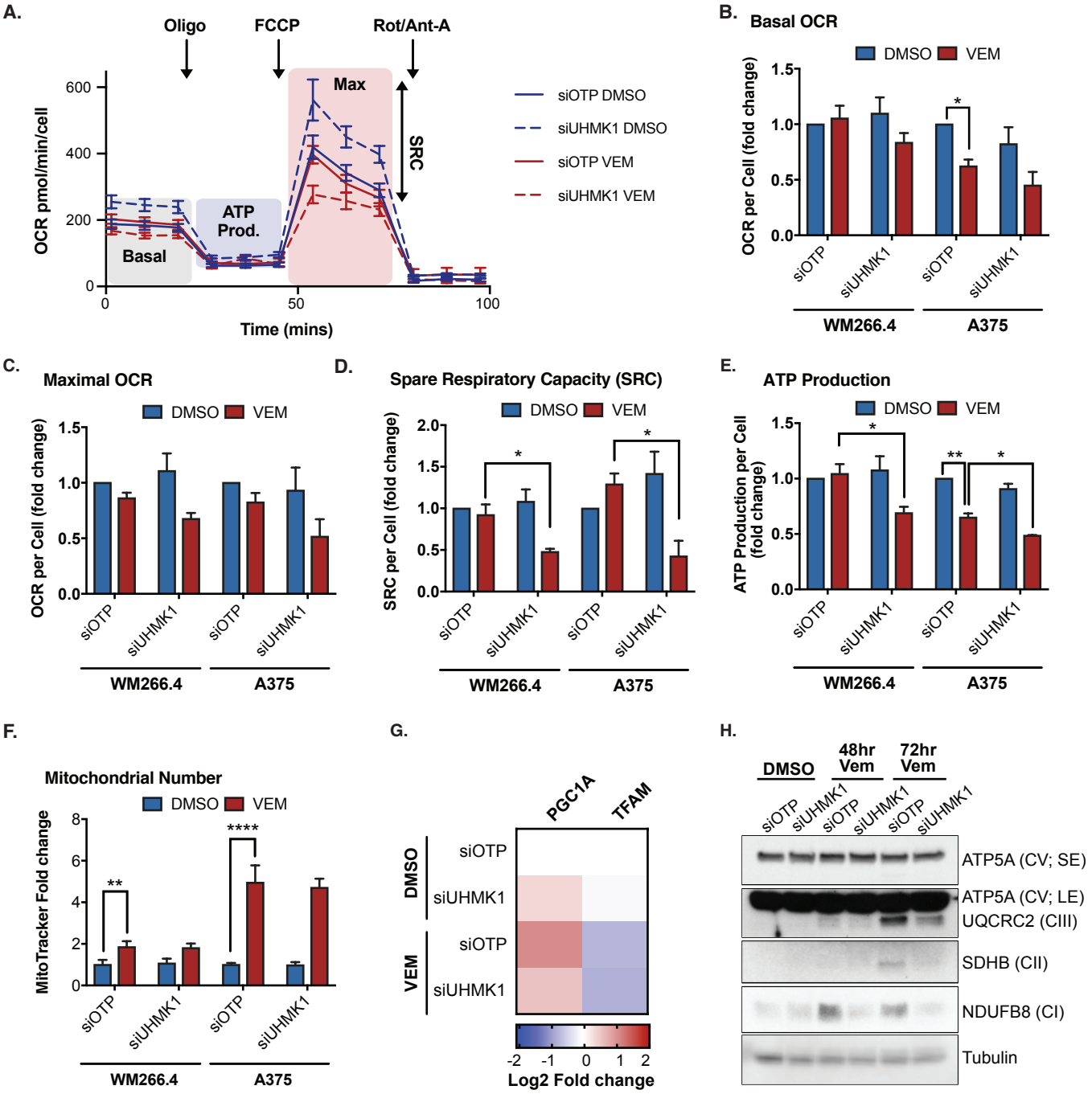

Figure 4. UHMK1 binds to mRNA encoding metabolic proteins and promotes selective mRNA transport in BRAF^{V600} melanoma cells adapting to BRAFi.

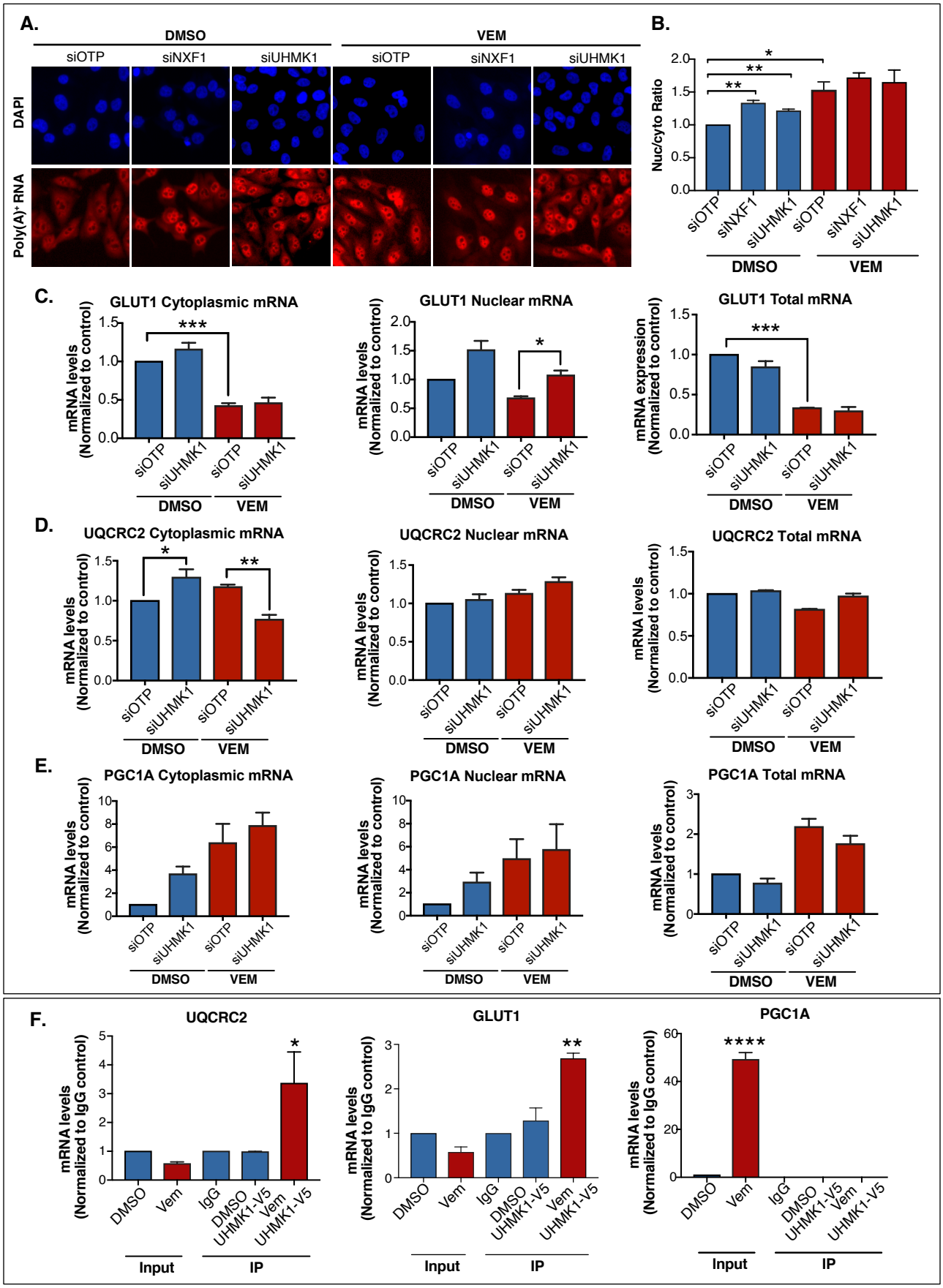

Figure 5. UHMK1 reprograms selective translation of mRNA encoding metabolic proteins folllowing BRAFi

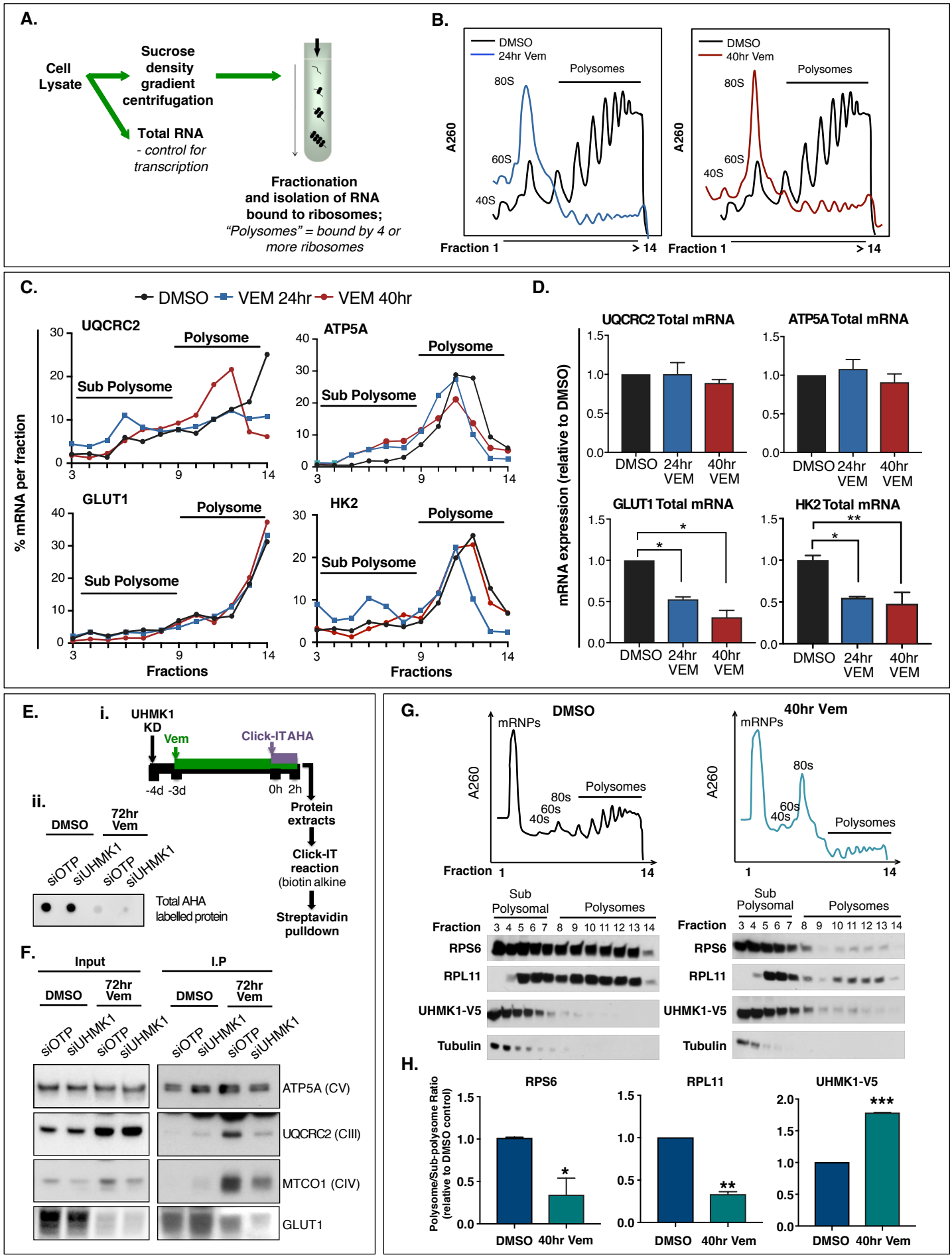

Figure 6. UHMK1 depletion sensitizes BRAFV600 melanoma cells to BRAF and MEK combination therapy *in vitro* and *in vivo*.

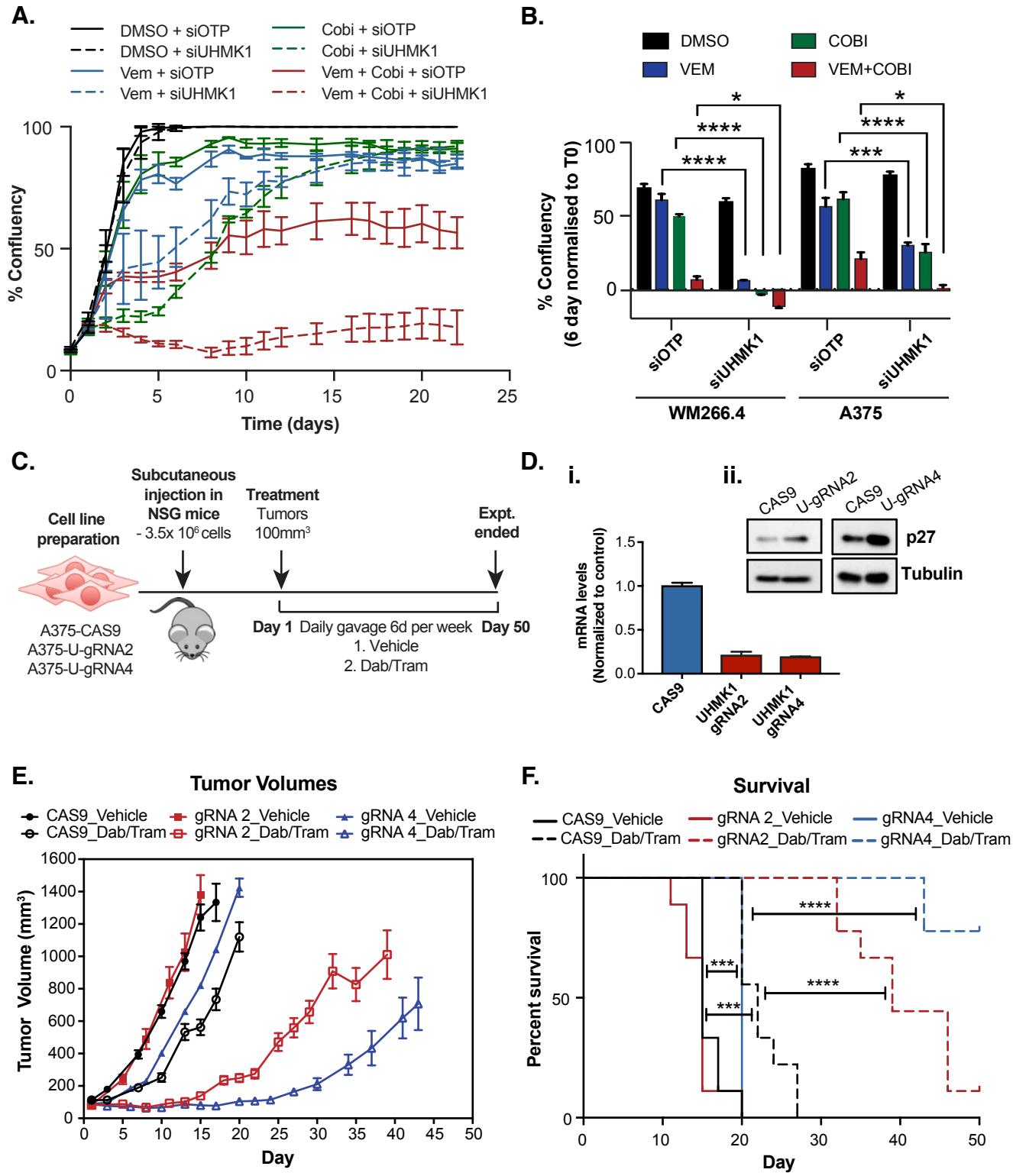
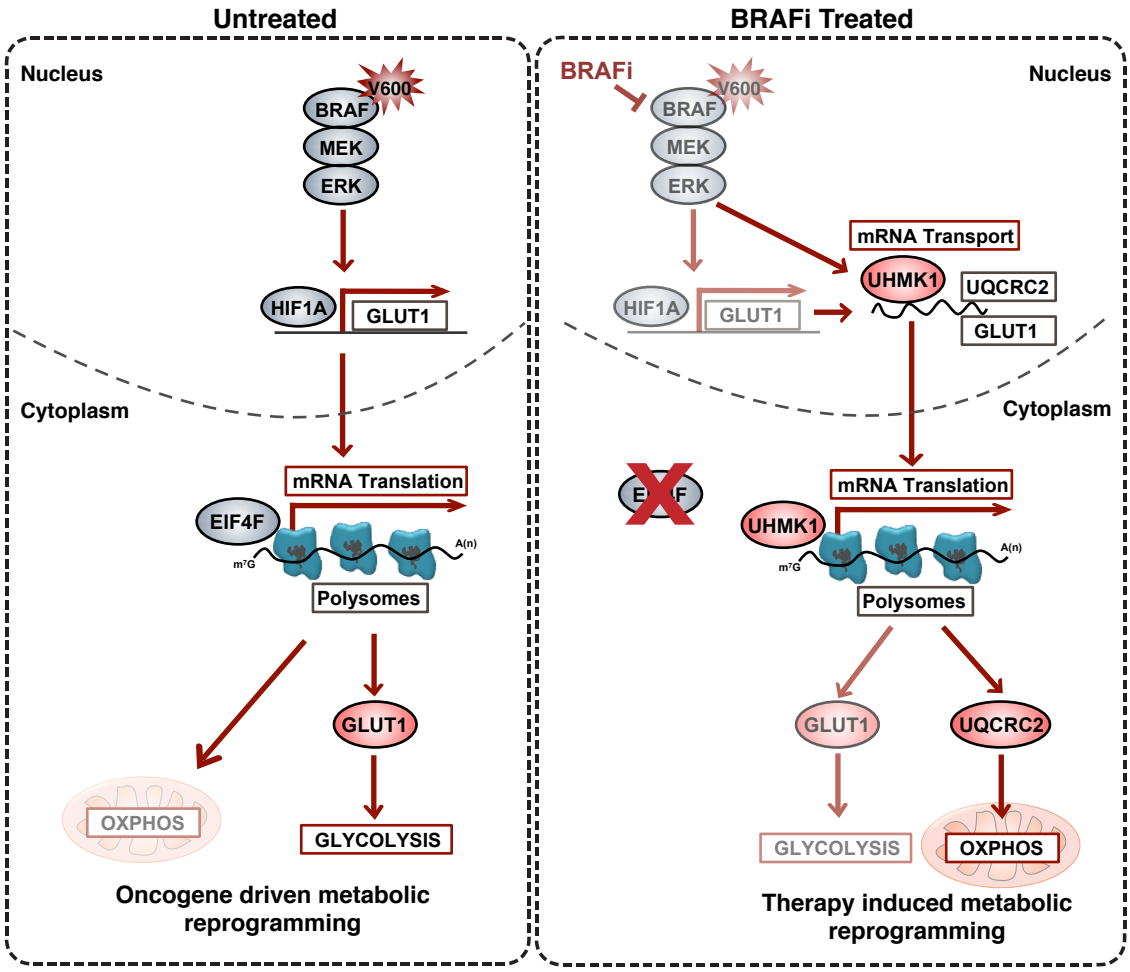
Figure 7. RNA binding kinase UHMK1 reprograms metabolism in response to BRAF inhibition via selective mRNA transport and translation